The Journal of Immunology

Paired Ig-like Receptor B Inhibits IL-13–Driven Eosinophil Accumulation and Activation in the Esophagus

Netali Ben Baruch-Morgenstern, Melissa K. Mingler, Emily Stucke, John A. Besse, Ting Wen, Hadar Reichman, Ariel Munitz and Marc E. Rothenberg

J Immunol 2016; 197:707-714; Prepublished online 20 June 2016;
doi: 10.4049/jimmunol.1501873
http://www.jimmunol.org/content/197/3/707

The Journal of Immunology is published twice each month by
The American Association of Immunologists, Inc.,
1451 Rockville Pike, Suite 650, Rockville, MD 20852

Print ISSN: 0022-1767 Online ISSN: 1550-6606.

Paired Ig-like Receptor B Inhibits IL-13–Driven Eosinophil Accumulation and Activation in the Esophagus

Netali Ben Baruch-Morgenstern,* Melissa K. Mingler,† Emily Stucke,† John A. Besse,† Ting Wen,† Hadar Reichman,* Ariel Munitz,*,[1] and Marc E. Rothenberg†,[1]

Eosinophilic esophagitis (EoE) is a Th2 cytokine–associated disease characterized by eosinophil infiltration, epithelial cell hyperplasia, and tissue remodeling. Recent studies highlighted a major contribution for IL-13 in EoE pathogenesis. Paired Ig-like receptor B is a cell surface immune-inhibitory receptor that is expressed by eosinophils and postulated to regulate eosinophil development and migration. We report that *Pirb* is upregulated in the esophagus after inducible overexpression of IL-13 (CC10-*Il13*^{Tg} mice) and is overexpressed by esophageal eosinophils. CC10-*Il13*^{Tg}/*Pirb*$^{-/-}$ mice displayed increased esophageal eosinophilia and EoE pathology, including epithelial cell thickening, fibrosis, and angiogenesis, compared with CC10-*Il13*^{Tg}/*Pirb*$^{+/+}$ mice. Transcriptome analysis of primary *Pirb*$^{+/+}$ and *Pirb*$^{-/-}$ esophageal eosinophils revealed increased expression of transcripts associated with promoting tissue remodeling in *Pirb*$^{-/-}$ eosinophils, including profibrotic genes, genes promoting epithelial-to-mesenchymal transition, and genes associated with epithelial growth. These data identify paired Ig-like receptor B as a molecular checkpoint in IL-13–induced eosinophil accumulation and activation, which may serve as a novel target for future therapy in EoE. ***The Journal of Immunology*****, 2016, 197: 707–714.**

Eosinophilic esophagitis (EoE) is an emerging inflammatory disease that is characterized by dominant eosinophilic inflammation, epithelial hyperplasia, collagen deposition, and tissue fibrosis (1, 2).

Patients with EoE have increased esophageal expression of IL-13, and ex vivo treatment of esophageal epithelial cells with IL-13 leads to dramatic gene expression alterations that are strikingly similar to those found in biopsies from patients with EoE (3). IL-13 is directly responsible for the induction of eosinophil-specific chemokines, such as those belonging to the eotaxin family. Chronic induction of IL-13 in the lungs using a doxycycline (DOX)-induced, CC10 promoter–regulated, IL-13–transgenic mouse model (*CC10-Il13*^{Tg}) leads to experimental EoE with typical esophageal pathology including eosinophil accumulation, fibrosis, epithelial cell hyperplasia, and angiogenesis (4, 5). Indeed, an anti–IL-13 therapeutic in patients with EoE markedly reverses the disease-specific transcriptome, including markers of tissue remodeling and chemokine expression, proving the centrality of the IL-13–induced response in EoE (6).

Although eosinophils likely promote EoE, pathways that limit eosinophil accumulation and/or activation in EoE are poorly defined. In fact, inhibitory checkpoints, particularly in the settings of IL-13–driven inflammation, have not been described. Accordingly, we aimed to define molecular pathways that regulate the activities of esophageal eosinophils, with specific emphasis on inhibitory, Ig-like receptors, which provide counterregulatory signals for various eosinophil activities (7). Paired Ig-like receptor (PIR)-B is a member of the Ig superfamily and is expressed primarily in a pairwise fashion with PIR-A on the surface of myeloid cells, including eosinophils (8, 9). PIR-B contains four ITIMs, which are capable of binding intracellular phosphatases, such as SHP-1 and/or SHP-2, and subsequently suppress cellular activation elicited by PIR-A, cytokines, chemokines, TLRs, and adhesion molecules (10–15). We demonstrated previously that PIR-B is a negative regulator of eotaxin-induced eosinophil chemotaxis and recruitment, as well as that the PIR-A/PIR-B axis plays a critical role in eosinophil development (13, 15). Although these data suggest key functions for PIR-B in eosinophil-associated pathologies, the role of PIR-B in EoE has not been defined. In this study, we demonstrate a key inhibitory function for PIR-B in EoE pathogenesis; overexpression of IL-13 in *Pirb*$^{-/-}$ mice leads to exaggerated EoE, including eosinophilic infiltration, epithelial cell thickening, fibrosis, and angiogenesis. Our results demonstrate that eosinophil activities in EoE are intrinsically suppressed by PIR-B and that loss of PIR-B by eosinophils mediates increased experimental EoE pathogenesis.

Materials and Methods

Mice

We generated bitransgenic mice (*CC10-Il13*^{Tg}) in which *Il13* was expressed in a lung-specific manner that allowed for external regulation of the transgene expression, as previously described (5). This model was specifically chosen because we showed previously that overexpression of IL-13 in the

*Department of Clinical Microbiology and Immunology, Sackler School of Medicine, Tel Aviv University, Ramat Aviv 69978, Israel; and †Division of Allergy and Immunology, Cincinnati Children's Hospital Medical Center, Cincinnati, OH 45229

[1]A.M. and M.E.R. contributed equally to this work.

ORCIDs: 0000-0001-6530-0387 (N.B.B.-M.); 0000-0003-1626-3019 (A.M.).

Received for publication August 21, 2015. Accepted for publication May 23, 2016.

This work was supported by the US-Israel Binational Science Foundation (Grant 2011244), the Israel Science Foundation (Grant 955/11), an Israel Cancer Research Foundation Research Career Development Award, and a Boaz and Varda Dotan Center Grant for Hemato-Oncology Research (all to A.M.); the US-Israel Binational Science Foundation (Grant 2009222 to A.M. and M.E.R.); and the National Institutes of Health National Institute of Allergy and Infectious Diseases (R01AI083450 and R37AI045898), the CURED Foundation, and the Buckeye Foundation (all to M.E.R.). This work was performed in partial fulfillment of the requirements for the Ph.D. degree of N.B.B.-M. at Tel Aviv University.

The data set in this article has been submitted to the Gene Expression Omnibus (http://www.ncbi.nlm.nih.gov/geo/query/acc.cgi?acc=GSE81135) under accession number GSE81135.

Address correspondence and reprint requests to Dr. Ariel Munitz or Dr. Marc E. Rothenberg, Department of Clinical Microbiology and Immunology, Sackler School of Medicine, Tel Aviv University, Ramat Aviv 69978, Israel (A.M.) or Division of Allergy and Immunology, Cincinnati Children's Hospital Medical Center, 3333 Burnet Avenue, Cincinnati, OH 45229 (M.E.R.). E-mail addresses: arielm@post.tau.ac.il (A.M.) or rothenberg@cchmc.org (M.E.R.)

The online version of this article contains supplemental material.

Abbreviations used in this article: BALF, bronchoalveolar lavage fluid; DOX, doxycycline; EoE, eosinophilic esophagitis; MBP, major basic protein; MFI, mean fluorescence intensity; PIR, paired Ig-like receptor; qPCR, quantitative PCR.

lungs induces esophageal disease resembling EoE (4). Male and female 6- to 8-wk-old *Pirb*$^{-/-}$ mice of generations > F9 were backcrossed to C57BL/6 mice (9). *CC10-Il13*^{Tg}*/Pirb*$^{-/-}$ and *CC10-Il13/Pirb*$^{+/+}$ mice were generated by breeding *CC10-Il13*^{Tg} mice with *Pirb*$^{-/-}$ mice. For all experiments, littermates were used as controls. We induced *Il13* transgene expression by feeding the *CC10-Il13*^{Tg} mice DOX-impregnated food (625 mg/kg; Purina Mills, Richmond, IN) for 2 wk. Animals were housed under specific pathogen–free conditions in accordance with institutional guidelines.

Real-time quantitative PCR

RNA samples from the whole esophagus were subjected to reverse-transcription analysis using SuperScript II reverse transcriptase (Invitrogen), according to the manufacturer's instructions. Quantitative PCR (qPCR) analysis was performed using the CFX96 system (Bio-Rad) in conjunction with the ready-to-use FastStart SYBR Green I Master reaction kit (Roche Diagnostic Systems). Results were normalized to *Hprt* cDNA, as previously described (16). The following primers were used in this study (5′–3′): *Ccl11* (encodes eotaxin-1), forward CACGGTCACTTCCTTCACG and reverse GGGGATCTTCTTACTGGTA; *Acta2* (encodes α-SMA), forward AGTCGCTGTCAGGAACCCTGAGAC and reverse CGAAGCCGGCCTTACAGAGCC; and *Hprt*, forward GTAATGATCAGTCAACGGGGGAC and reverse CCAGCAAGCTTGCAACCTTAACCA.

Flow cytometry

Flow cytometric analysis of bone marrow, peripheral blood cells, or enzymatically digested esophagus was conducted using the following Abs: anti-CD11b (R&D Systems, Minneapolis, MN), anti–GR-1 (BD Bioscience), anti–Siglec-F (BD Bioscience), anti-CCR3 (BD Bioscience), anti–PIR-A/B (eBioscience), IgG2b (eBioscience), anti-CD45 (eBioscience), and anti-CD11c (BD Bioscience). Cell counts were conducted using 123count eBeads (eBioscience), according to the manufacturer's instructions. In all experiments, ≥50,000 events were acquired using a FACSCalibur (BD Bioscience), and data were analyzed using Kaluza (Beckman Coulter) or FlowJo (TreeStar) software.

Phosphoflow

Total bone marrow cells were stained with anti-CD45 (eBioscience), anti–Siglec-F, and anti-CCR3 (both from BD Bioscience). Mature eosinophils (triple positive) were sorted using a MoFlo XDP (Beckman Coulter). The cells were activated with bronchoalveolar lavage fluid (BALF), which was obtained from the lungs of *CC10-Il13*^{Tg}*/Pirb*$^{+/+}$ mice, for the indicated times (0, 5, and 10 min), and cells were fixed in 4% paraformaldehyde/PBS and permeabilized using saponin-based permeabilization buffer (X1; Invitrogen). Cells were stained with phospho-ERK1/2 (Cell Signaling). Events were acquired using a FACSCanto (BD Bioscience), and data were analyzed using Kaluza (Beckman Coulter) or FlowJo (TreeStar) software. For phosphoflow analysis, the mean fluorescence intensity (MFI) for each time point, in each biological repeat, was normalized to baseline and expressed as the fold change over baseline.

ELISA

IL-13 and CCL11 levels were assessed using commercial ELISA kits (DuoSet; R&D Systems), according to the manufacturer's instructions. The lower detection limits for IL-13 and CCL11 were 62.5 and 15.6 pg/ml, respectively.

Quantifying tissue eosinophils by major basic protein staining

Esophageal or lung eosinophils were detected using an immunohistochemical stain against murine eosinophilic major basic protein (MBP), as previously described (4). Quantification of positive cells was performed using Cell^A imaging software, and results were reported as immunoreactive cells/mm^2.

Epithelial thickness and collagen quantification

Epithelial thickness was determined for cross-sectioned esophageal samples using MBP stain. Quantification of thickness was performed using Cell^A imaging software by taking 7–14 lengthwise measurements/slide from the lumen to the basement membrane of each esophagus. Collagen deposition was determined by staining esophageal samples with Masson's trichrome and quantified using Cell^A software. Collagen measurements were recorded as area of collagen staining/length of basement membrane, as previously described (4).

Assessing angiogenesis

Tissues were fixed, embedded, sectioned, prepared, and stained as previously described (4). Morphometry was used to determine the average number of CD31$^+$ vessels/high-power field in each group.

Affymetrix cDNA microarray

Mouse Affymetrix (Santa Clara, CA) microarrays (2.0 ST GeneChip) were performed and analyzed using established protocols of the Cincinnati Children's Hospital Medical Center Gene Expression Core and according to the manufacturer's instructions. Data were analyzed using GeneSpring software, with a fold-change cutoff of 2 and unpaired Student *t* test ($p > 0.05$). Heat plots and Venn diagrams were created according to gene lists that were generated using GeneSpring software (Agilent, Santa Clara, CA).

Eosinophil depletion

CC10-Il13^{Tg}*/Pirb*$^{-/-}$ and *CC10-Il13/Pirb*$^{+/+}$ mice were fed with DOX for 2 wk. They were injected i.p. with 20 μg soluble anti-mouse Siglec-F on days −1, 1, 4, 7, and 10; Rat IgG2a was used as an isotype-matched control Ab (R&D Systems) (17). At day 14, the mice were sacrificed, and the esophagus was analyzed for eosinophil levels using anti-MBP staining. Epithelial thickness, collagen deposition, and *Acta2* transcript levels were determined, as described above.

Statistical analysis

Data were analyzed by the Student *t* test or by ANOVA followed by the Tukey post hoc test using GraphPad Prism 5. Data are shown as mean ± SEM, and *p* values < 0.05 were considered statistically significant.

Results

Pirb *is an IL-13–induced, eosinophil-associated gene in the esophagus*

Pirb expression was increased in the esophagus following *Il13* transgene induction (Fig. 1A). To define the cellular source accounting for increased *Pirb* expression, polychromatic flow cytometric staining was conducted using single-cell suspensions of esophageal tissue. After overexpression of IL-13, eosinophils constituted the largest PIR-A/B$^+$ cellular source in the esophagus, reaching nearly 40% of the entire CD45$^+$ cellular population, whereas neutrophil and CD11C$^+$/GR1$^-$ cell populations were ∼7 and ∼4%, respectively. Importantly, the second major CD45$^+$ population (>15%), the lymphocyte population, did not express PIR-A/B (Fig. 1B, 1C, Supplemental Fig. 1). Furthermore, among the CD45$^+$ cell population, eosinophils expressed relatively high surface levels of PIR-A/B (Fig. 1C). Notably, PIR-A/B expression in the esophagus was confined to the hematopoietic compartment because CD45$^-$ cells did not express PIR-A/B (Fig. 1D). Interestingly, the expression of PIR-A/B on esophageal eosinophils was higher than that found on peripheral blood eosinophils (Fig. 1E). Thus, increased expression of PIR-B in the esophagus after IL-13 induction is attributable to infiltration of inflammatory cells, especially eosinophils.

PIR-B negatively regulates IL-13–driven esophageal eosinophilia

To define the role of PIR-B in IL-13–induced esophageal pathology, *Pirb*$^{-/-}$ mice were mated with *CC10-Il13*^{Tg} mice to generate *CC10-Il13*^{Tg}*/Pirb*$^{-/-}$ and *CC10-Il13*^{Tg}*/Pirb*$^{+/+}$ mice. Thereafter, the mice were fed with DOX for 2 wk, and eosinophil infiltration into the esophagus was determined. *CC10-Il13*^{Tg}*/Pirb*$^{+/+}$ mice displayed increased eosinophil accumulation in the esophagus, as assessed by antieosinophil MBP staining (Fig. 2A, 2B) and flow cytometric analysis of CD45$^+$/CD11b$^+$/Siglec-F$^+$/SSC^{hi} cells (Fig. 2C). DOX-treated *CC10-Il13*^{Tg}*/Pirb*$^{-/-}$ mice displayed a nearly 2-fold increase in the levels of esophageal eosinophilia in comparison with DOX-treated *CC10-Il13*^{Tg}*/Pirb*$^{+/+}$mice (Fig. 2D). This increase is impressive considering the already marked increased eosinophilia in the esophagus and lungs of *CC10-Il13*^{Tg} mice (3). Moreover, the *Pirb*$^{-/-}$ eosinophil population was ∼60% of the entire CD45$^+$ cell population. Other examined CD45$^+$ cell populations did not increase, which demonstrates that the inhibitory regulatory role of PIR-B in the accumulation of CD45$^+$ cells is specific to eosinophils (Fig. 2E, Supplemental Fig. 2). Increased

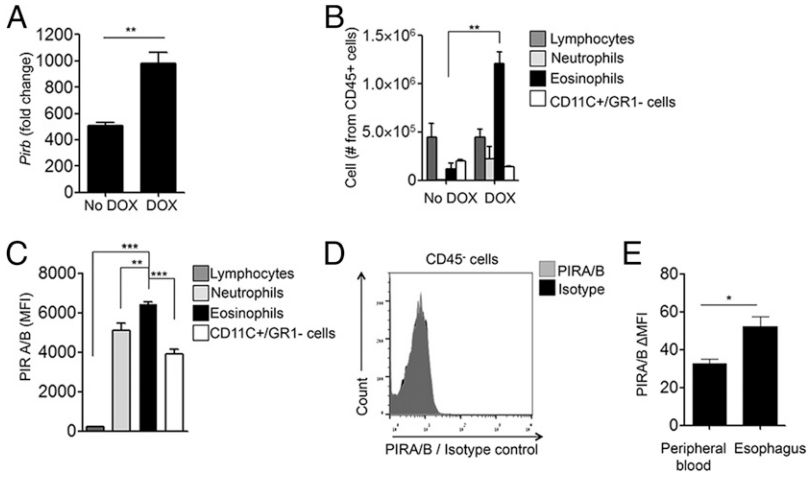

FIGURE 1. Expression of PIR-B in IL-13–induced experimental EoE. (**A**) The expression of *Pirb* was assessed by microarray analysis in the esophagus of *CC10-Il13*^{Tg} mice after 2 wk of DOX or no DOX feeding. (**B**) Flow cytometric analysis of the main cellular populations infiltrating the esophagus after IL-13 overexpression. (**C**) Analysis of PIR-A/B surface expression in various cell types after DOX treatment. ΔMFI for PIR-A/B expression was calculated by subtracting the MFI obtained for anti–PIR-A/B staining from that obtained for the isotype control. (**D**) Representative plot of PIR-B expression by esophageal CD45^{-} cells. (**E**) Analysis of surface PIR-A/B expression in peripheral blood eosinophils and esophageal eosinophils. Data in (A)–(C) and (E) are mean + SEM. Data are from three to five mice for each group. $^{*}p < 0.05$, $^{**}p < 0.01$, $^{***}p < 0.001$.

eosinophil infiltration was not confined to the esophagus, because analysis of anti-MBP–stained lung specimens and differential cell counts from BALF reveled increased lung eosinophilia in DOX-treated *CC10-Il13*^{Tg}*/Pirb*$^{-/-}$ mice in comparison with *CC10-Il13*^{Tg}*/Pirb*$^{+/+}$ mice (Supplemental Fig. 3). Furthermore, increased eosinophil infiltration into the esophagus and lungs of DOX-treated *CC10-Il13*^{Tg}*/Pirb*$^{-/-}$ mice was not due to alterations in IL-13 or eosinophil chemoattractant expression, because BALF and esophageal levels of IL-13 and CCL11 were similar in DOX-treated *CC10-Il13*^{Tg}*/Pirb*$^{-/-}$ and *CC10-Il13*^{Tg}*/Pirb*$^{+/+}$ mice (Fig. 2F–H).

PIR-B inhibits the development of IL-13–induced esophageal pathology

The elevated levels of eosinophils in the esophagus of DOX-treated *CC10-Il13*^{Tg}*/Pirb*$^{-/-}$ mice suggested a possible role for PIR-B in regulating IL-13–induced esophageal pathology. Masson's trichrome staining revealed increased areas of esophageal collagen deposition in DOX-treated *CC10-Il13*^{Tg}*/Pirb*$^{-/-}$ mice (Fig. 3A, 3B). Furthermore, qPCR analysis of *Acta2* expression, a prototype marker of myofibroblasts, revealed substantially increased *Acta2* expression in DOX-treated *CC10-Il13*^{Tg}*/Pirb*$^{-/-}$ mice (Fig. 3C). Moreover, the epithelial cell layer was significantly increased in DOX-treated *CC10-Il13*^{Tg}*/Pirb*$^{-/-}$ mice (Fig. 3D). Assessment of IL-13–induced blood vessel formation using anti-CD31 staining revealed greater vessel size (Fig. 3E) and quantity (Fig. 3F) in DOX-treated *CC10-Il13*^{Tg}*/Pirb*$^{-/-}$ mice than DOX-treated *CC10-Il13*^{Tg}*/Pirb*$^{+/+}$ mice.

PIR-B inhibits IL-13–induced eosinophil-dependent collagen deposition and angiogenesis

We hypothesized that PIR-B inhibits IL-13–mediated eosinophil-dependent increased tissue remodeling, as seen in *CC10-Il13*^{Tg}*/Pirb*$^{-/-}$ mice. To test this hypothesis, we injected anti-Siglec-F–specific Abs,

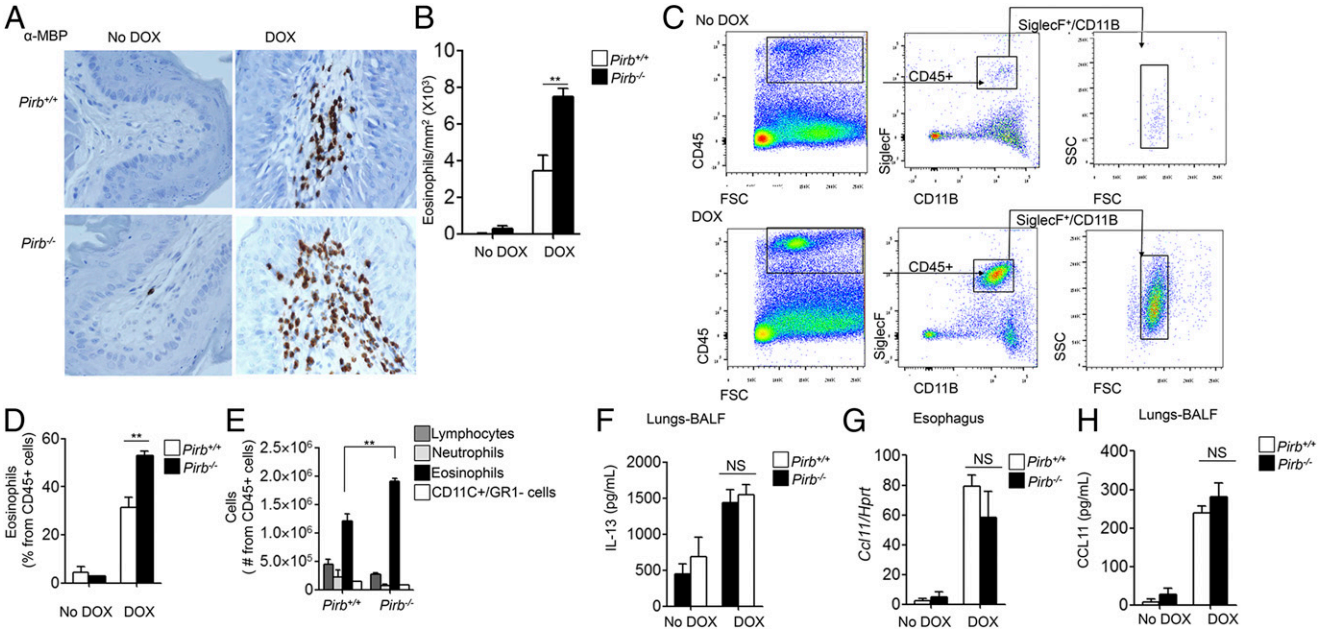

FIGURE 2. Eosinophil levels in the esophagus of *CC10-Il13*^{Tg}*/Pirb*$^{-/-}$ mice. *CC10-Il13*^{Tg}*/Pirb*$^{-/-}$ and *CC10-Il13*^{Tg}*/Pirb*$^{+/+}$ mice were treated or not with DOX for 2 wk. Thereafter, the mice were sacrificed, and the esophageal tissue was used for histology (**A** and **B**) or flow cytometric analysis (**C**). Representative photomicrograph [(A), original magnification ×400] and quantitation (B) of antieosinophil MBP immunohistochemical stain. Representative gating strategy (**C**) and quantification (**D**) of esophageal eosinophils from mice treated or not with DOX, as determined by flow cytometry. (**E**) Flow cytometric analysis of the main cellular populations infiltrating the esophagus after IL-13 overexpression. Lung and esophageal IL-13 (**F**) and CCL11 (**H**) protein expression levels, as well as expression of esophageal *Ccl11* transcripts [(**G**), fold over housekeeping gene]. Data are from two or three independent experiments in which $n = 2$ for each of the groups not treated with DOX and $n = 4$ for each of the DOX-treated groups. Data in (B) and (D)–(H) are mean + SEM. $^{**}p < 0.01$.

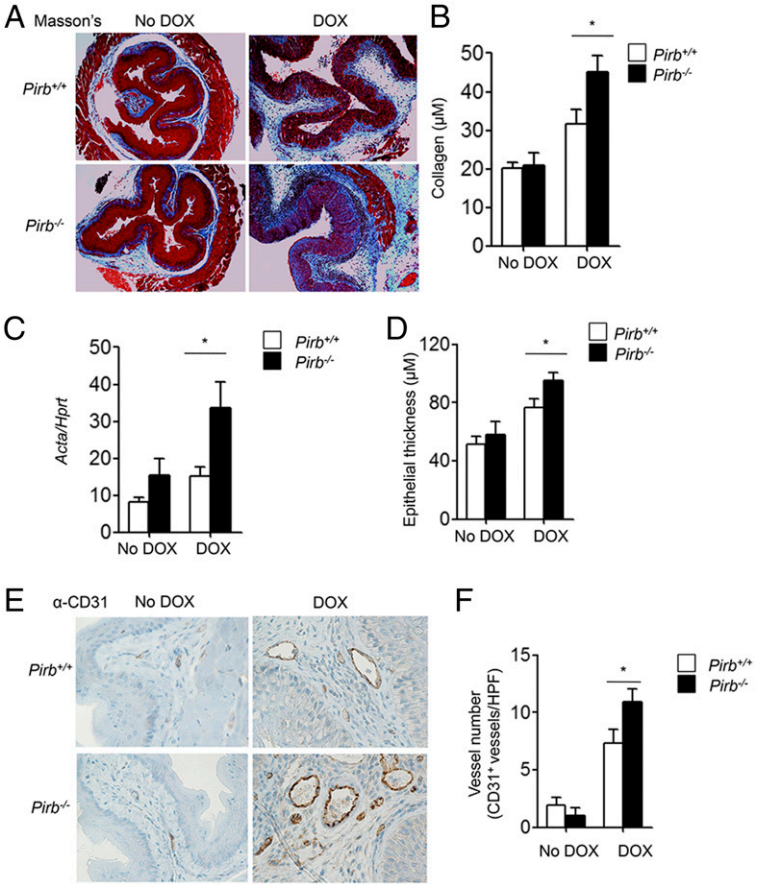

FIGURE 3. Esophageal tissue remodeling in *CC10-Il13*^{Tg}*/Pirb*$^{-/-}$ mice. *CC10-Il13*^{Tg}*/Pirb*$^{-/-}$ and *CC10-Il13*^{Tg}*/Pirb*$^{+/+}$ mice were treated or not with DOX for 2 wk. Thereafter, the mice were sacrificed, and the esophageal tissues were obtained. Representative photomicrographs of Masson's trichrome staining [(**A**), original magnification ×400] and morphometric and quantitative analysis of collagen deposition (**B**). (**C**) α-Smooth muscle actin gene expression (*Acta2*) in the esophagus was determined by qPCR analysis and normalized to the housekeeping gene *Hprt*. (**D**) Quantitative analysis of epithelial cell thickness. Morphometric (**E**) and quantitative (**F**) analysis of anti-CD31 staining per high power field (HPF). Original magnification ×100. Data were obtained from three independent experiments, with ≥4 mice for each group. Data in (B)–(D) and (F) are mean + SEM. *$p < 0.05$.

which are known to induce eosinophil apoptosis (17, 18), and monitored esophageal pathology. Anti–Siglec-F treatment resulted in complete depletion of esophageal eosinophils in DOX-treated *CC10-Il13*^{Tg}*/Pirb*$^{+/+}$ and *CC10-Il13*^{Tg}*/Pirb*$^{-/-}$ mice (Supplemental Fig. 4). If the worsened pathology in *CC10-Il13*^{Tg}*/Pirb*$^{-/-}$ mice was dependent on the expression of PIR-B in eosinophils, depletion of eosinophils in DOX-treated *CC10-Il13*^{Tg}*/Pirb*$^{-/-}$ mice should result in a similar severity of pathology as in *CC10-Il13*^{Tg}*/Pirb*$^{+/+}$ mice. Indeed, assessment of esophageal pathology in eosinophil-depleted, DOX-treated *CC10-Il13*^{Tg}*/Pirb*$^{-/-}$ and *CC10-Il13*^{Tg}*/Pirb*$^{+/+}$ mice revealed that, in the absence of eosinophils, *CC10-Il13*^{Tg}*/Pirb*$^{-/-}$ and *CC10-Il13*^{Tg}*/Pirb*$^{+/+}$ mice displayed similar pathology in terms of collagen deposition and angiogenesis (as revealed by Masson's trichrome staining and anti-CD31 staining) (Fig. 4A–D). Notably, eosinophil depletion did not prevent the increased epithelial thickness and increased *Acta2* expression in DOX-treated *CC10-Il13*^{Tg}*/Pirb*$^{-/-}$ mice, indicating that PIR-B may regulate the activities of additional non-eosinophil cells that are responsible for these aspects of tissue remodeling (Fig. 4E).

PIR-B inhibits IL-13–mediated eosinophil activation

We hypothesized that PIR-B may serve as an intrinsic inhibitor of eosinophil activation in the esophagus. To assess this possibility, we examined the activation (i.e., phosphorylation) status of ERK in eosinophils (as a surrogate marker for eosinophil activation) in response to the inflammatory milieu, which is elicited by IL-13. To this end, naive primary eosinophils were sorted from the bone marrow of *CC10-Il13*^{Tg}*/Pirb*$^{-/-}$ and *CC10-Il13*^{Tg}*/Pirb*$^{+/+}$ mice. Thereafter, the cells were activated with BALF obtained from the lungs of DOX-treated *CC10-Il13*^{Tg}*/Pirb*$^{+/+}$ mice. Eosinophils activated with BALF from *CC10-Il13*^{Tg}*/Pirb*$^{+/+}$ mice had readily detectable phosphorylation of ERK (~1.25-fold increase over baseline). In contrast, activation of *Pirb*$^{-/-}$ eosinophils resulted in substantially greater ERK phosphorylation (~1.9-fold increase over baseline, Fig. 5) than did activation of *Pirb*$^{+/+}$ eosinophils. These data demonstrate that PIR-B is an intrinsic negative regulator of eosinophil activation in response to the IL-13–induced microenvironment.

PIR-B negatively regulates IL-13–induced esophageal eosinophil effector functions

Next, we aimed to define the transcriptome signature of *Pirb*$^{+/+}$ and *Pirb*$^{-/-}$ esophageal eosinophils. To this end, microarray analysis was performed on primary eosinophils that were sorted from the bone marrow and esophagus of DOX-treated *CC10-Il13*^{Tg}*/Pirb*$^{+/+}$ and *CC10-Il13*^{Tg}*/Pirb*$^{-/-}$ mice (the complete data set can be found at http://www.ncbi.nlm.nih.gov/geo/query/acc.cgi?acc=GSE81135).

To determine whether local overexpression of IL-13 exerts any systemic effects on bone marrow eosinophils, bone marrow eosinophils were obtained and subjected to microarray analysis. Elevated expression of IL-13 resulted in modest effects on *Pirb*$^{+/+}$ bone marrow eosinophils; it induced alteration of 76 genes (55 upregulated genes and 21 downregulated genes; Fig. 6A, gene lists 1 and 2 online). In contrast, IL-13 induced marked alterations in *Pirb*$^{+/+}$ esophageal eosinophils (Fig. 6A); there was an ~8-fold increase in the total amount of upregulated genes in esophageal eosinophils (433 genes) compared with bone marrow eosinophils (Fig. 6A, gene lists 3 and 4 online). These genes included multiple cell surface receptors: cytokine and chemokine receptors (e.g., *Ccrl2*, *Il1r2*, *Ccr1*, and *Csf2rb2*), Ig-like receptors (e.g., *Lilrb3/Pirb*, *Lilra6/Pira*, *Cd300lf*, *Cd300ld*, *Cd300lb*, and *Gp49a*), and cell adhesion and migration molecules (e.g., *Cd44*, *Itga2*, and *Itga4*). In addition, various enzymatic pathways (e.g., *Ptgs2*, *Ear11*, *Adam8*, and *Mmp25*) and secreted factors, such as cytokines (e.g., *Il1a*, *Il1b*,

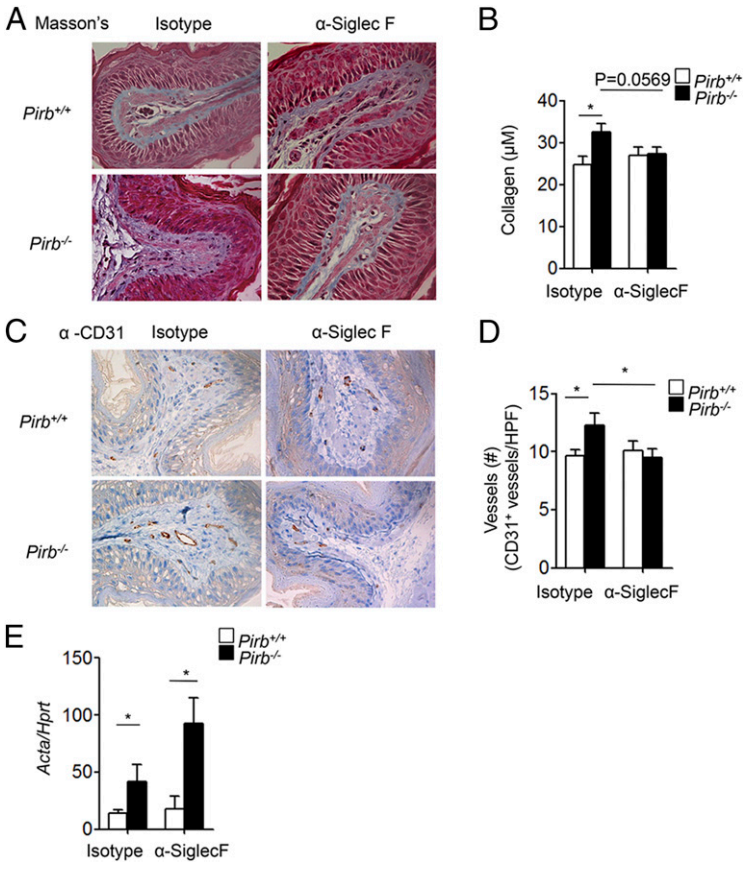

FIGURE 4. Eosinophil-dependent esophageal tissue remodeling in *CC10-Il13^{Tg}/Pirb$^{-/-}$* mice. *CC10-Il13^{Tg}/Pirb$^{-/-}$* and *CC10-Il13^{Tg}/Pirb$^{+/+}$* mice were treated with DOX for 2 wk. Anti–Siglec F (or suitable isotype control) was injected into the peritoneal cavity on days −1, 0, 1, 4, 7, and 10. The mice were sacrificed on day 14, and esophageal tissues were obtained. Representative photomicrographs of Masson's trichrome stain (**A**) and anti-CD31 stain (**C**) (original magnification ×400). Quantitative analysis of collagen deposition (**B**) and the number of blood vessels in the esophagus per high power field (HPF) (**D**). (**E**) Expression of α-smooth muscle actin (*Acta2*) in the esophagus was determined by qPCR analysis and normalized to the housekeeping gene *Hprt*. Data are from five or six mice for each group. Data in (B), (D), and (E) are mean + SEM. *$p < 0.05$.

and *Il4*), chemokines (e.g., *Cxcl2*, *Ccl3*, *Ccl2*, *Ccl4*, and *Csf1*), and profibrogenic molecules (e.g., *Rentla*, *Retnlg*, *Postn*, and *Tnfaip3*), were upregulated. Moreover, IL-13 altered the expression of numerous intracellular signaling molecules (e.g., MAPK pathway [*Mapk6*, *Mapkapk2*, and *Mapk1ip1*], *JunB*, Nfkb pathway [*Nfkbiz*, *Nfkbia*, and *Nfkbie*], and transcription factors [*Cebpb*]). Finally, IL-13 induced a pronounced effect on the expression of *Pirb$^{+/+}$*eosinophil microRNAs (e.g., *Mir21*, *Mir1931*, and *Mir146b*), cell cycle–related molecules (e.g., *G0S2*, *cyclinG2*, *Gadd45a*, *S100a10*, and *S100a4*), and survival molecules (e.g., *Bcl2l11* and *Fas*) (Table I). Collectively, these data suggest a profound impact of IL-13 on esophageal eosinophils in the presence of PIR-B.

IL-13 had a dramatic effect on primary esophageal *Pirb$^{+/+}$* eosinophils. Nonetheless, primary esophageal eosinophils that were sorted from *CC10-Il13^{Tg}/Pirb$^{-/-}$* mice displayed a substantial hyperactivated phenotype in comparison with primary esophageal eosinophils that were sorted from *CC10-Il13^{Tg}/Pirb$^{+/+}$* mice (Fig. 6B versus Fig. 6A, *right panels*). For example, *Pirb$^{-/-}$* esophageal eosinophils showed induction of nearly 2-fold more genes than did *Pirb$^{+/+}$* esophageal eosinophils (854 and 433 genes, respectively) (Fig. 6A, 6B, gene lists 5 and 6). Importantly, altered gene expression in *Pirb$^{-/-}$* esophageal eosinophils was not due to systemic effects of IL-13, because *Pirb$^{-/-}$* bone marrow eosinophils from *CC10-Il13^{Tg}/Pirb$^{-/-}$* mice showed minimal gene alterations after induction of IL-13 (lists 7 and 8 online), and these alterations were similar to those observed in *Pirb$^{+/+}$* cells.

Analysis of the 854 genes that were induced in *Pirb$^{-/-}$* eosinophils revealed that the majority of these genes was also induced in wild-type eosinophils (354 of 433 genes, making up 82% of the IL-13–activated esophageal eosinophil transcriptome) (Fig. 6C, gene list 9 online). Importantly, among these 354 common genes, 30 were upregulated >2-fold in *Pirb$^{-/-}$* esophageal eosinophils, including various surface molecules (e.g., *Ccr1* and *Lilra6*), enzymes (e.g., *Adamdec1* and *Pla2g7*), secreted factors (e.g., *Retnla*, *Cxcl3*, and *Csf1*), and intracellular signal molecules (e.g., *Btg2* and *Irg1*) (Fig. 6D, Table II, gene list 10 online).

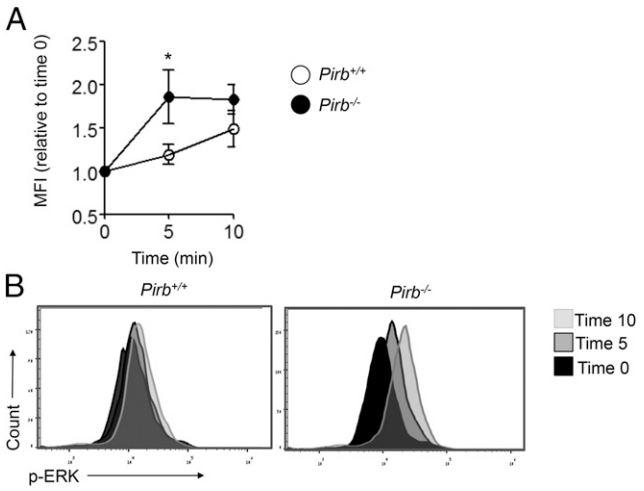

FIGURE 5. The role of PIR-B in eosinophil activation in response to the esophageal microenvironment. Primary naive mature (i.e., CD45^{+}/CCR3^{+}/Siglec-F^{+}/SSC^{hi}) bone marrow eosinophils were sorted from *CC10-Il13^{Tg}/Pirb$^{-/-}$* and *CC10-Il13^{Tg}/Pirb$^{+/+}$* mice and activated with BALF from DOX-treated CC10-*Il13^{Tg}/Pirb$^{+/+}$* mice for the indicated time. Phosphorylation of ERK1/2 was determined by phosphoflow analysis. (**A**) Kinetics. (**B**) Graphic representation of data. Data are from four mice for each group. *$p < 0.05$.

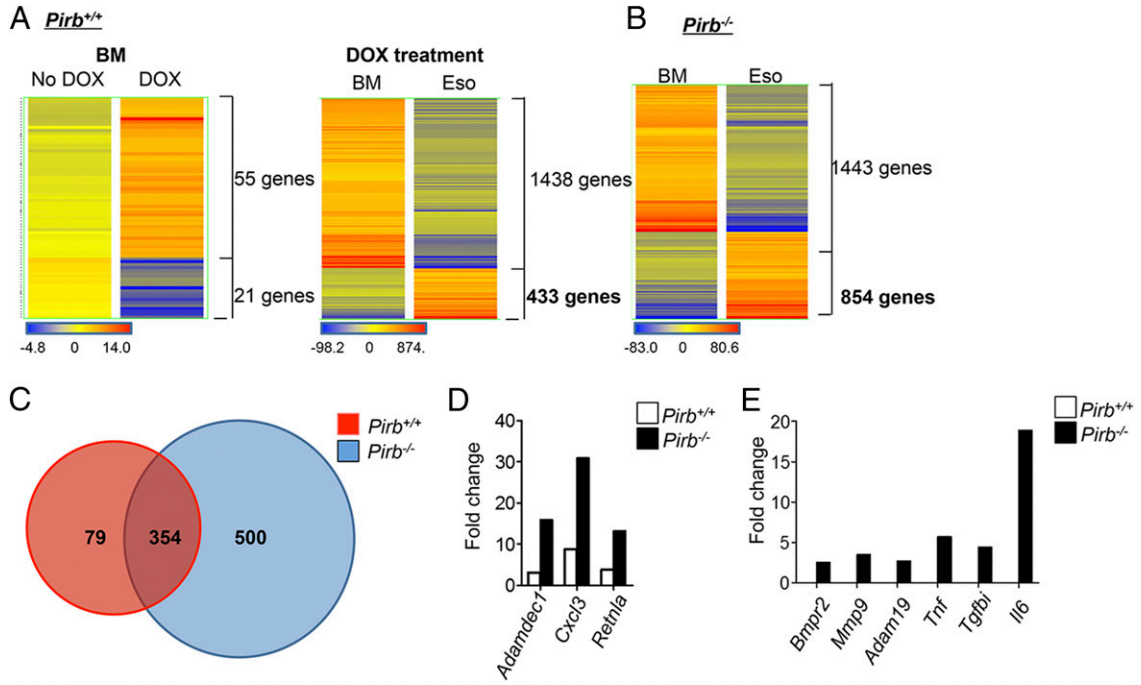

FIGURE 6. Gene expression profile in esophageal eosinophils after IL-13–induced experimental EoE. *CC10-Il13^{Tg}/Pirb$^{-/-}$* and *CC10-Il13^{Tg}/Pirb$^{+/+}$* mice were treated or not with DOX for 2 wk. Thereafter, the mice were sacrificed, and eosinophils were sorted from the esophagus and bone marrow and subjected to microarray analysis. (**A**) Heat plot analysis comparing *Pirb$^{+/+}$* bone marrow (BM) eosinophils from mice treated or not with DOX (*left panel*). Heat plot analysis of DOX-treated BM and esophageal (Eso) *Pirb$^{+/+}$* eosinophils (A, *right panel*) and *Pirb$^{-/-}$* eosinophils (**B**). (**C**) Venn diagram of the upregulated genes in DOX-treated esophageal *Pirb$^{+/+}$* and *Pirb$^{-/-}$* eosinophils. (**D**) Representative genes that were upregulated in esophageal eosinophils compared with bone marrow eosinophils from *CC10-Il13^{Tg}/Pirb$^{+/+}$*and *CC10-Il13^{Tg}/Pirb$^{-/-}$* mice. (**E**) Representative genes that were exclusively upregulated in esophageal eosinophils compared with bone marrow eosinophils from *CC10-Il13^{Tg}/Pirb$^{-/-}$* mice. Data are from three mice from each group with inclusion criteria of $p > 0.05$ and fold change > 2.

Further analysis revealed that *Pirb$^{-/-}$* esophageal eosinophils displayed a distinct genetic signature involving an exclusive upregulation of 500 additional genes (gene list 11 online). These genes included cell surface molecules, such as cytokine receptors (e.g., *Il5ra*, *Il12rb2*, *Ifnar1*, and *Bmpr2*), inhibitory receptors (e.g., *Cd300a*), and cell adhesion and migration molecules (e.g., *Itgax*, *Itgb3*, *Itgal*, *Ezr*, *acta1*, *Vasp*, and *Cd24*) (Fig. 6E). In addition, gene expression of various enzymatic pathways (e.g., *Mmp9*, *Capn2*, and *Adam19*), secreted factors (e.g., *Il6*, *Tnf*, *Cxcl10*, *Tgfbi*, *Areg*, and *Ccl8*), and receptors (e.g., *Notch1* and *Notch2*) that have been linked with tissue fibrosis was increased in *Pirb$^{-/-}$* eosinophils (Fig. 6E). Moreover, gene expression of intracellular signaling molecules, including key molecules of the IL-4/IL-13 signaling pathway (e.g., *Stat6*, *Jak2*), NF-κB signaling pathway (e.g., Nfkb2, *Rela*, *Nfkbib*), and signaling pathways that are involved in healing responses (e.g., *Jun*, *Fosl1*, *Tnik*, and *Irak2*), were elevated. Finally, genes of additional microRNAs (e.g., *Mir142* and *Mir1957*), as well as cell cycle (*Gadd45b* and *S100a6*) and survival molecules (e.g., *Bcl10*), had elevated expression (Table III).

Discussion

IL-13 is a key Th2 cytokine that can directly promote many of the disease features associated with EoE, including eosinophil infiltration and esophageal remodeling. Most studies focused on downstream effects of IL-13, and substantially less is known about the negative regulators of IL-13–induced esophageal pathology. In this study, we establish PIR-B as a novel inhibitory pathway that suppresses IL-13–induced eosinophil accumulation and subsequent activation in the esophagus. We demonstrated that the expression of *Pirb* is increased in the esophagus after exposure to IL-13; eosinophils are the predominant contributors to the increased PIR-A/B expression in EoE; PIR-B inhibits the development of IL-13–induced esophageal pathology, including eosinophilic accumulation, epithelial cell hyperplasia, collagen deposition, increased *Acta2* levels, and angiogenesis; eosinophil-depletion experiments suggest that increased collagen deposition and angiogenesis in response to IL-13 in *CC10-Il13^{Tg}/Pirb$^{-/-}$* mice are likely due to loss of negative regulation in esophageal eosinophils; and *Pirb$^{-/-}$* esophageal eosinophils display a distinct genetic signature associated with tissue repair. Collectively, our data establish PIR-B as an intrinsic negative regulator of eosinophil functions in IL-13–driven experimental EoE. This experimental finding may have implications for human EoE, which is characterized by IL-13–driven responses, as demonstrated by recent findings using anti–IL-13 treatment of patients with EoE (6).

We established that, following aeroallergen challenge, *Pirb$^{-/-}$* mice display decreased lung eosinophilia and that PIRs critically regulate eosinophil maturation and expansion in homeostasis and in settings of aeroallergen-induced asthma (13). Subsequently, allergen-induced eosinophil infiltration into the lungs is decreased. In contrast, IL-13–induced eosinophil levels in the lung and esophageal compartment are elevated. This finding is likely due to the fact that the regulation of eosinophil functions by PIRs is confined to a particular anatomical location and specifically regulates IL-5–induced eosinophilpoiesis. For example, the role of PIRs in eosinophil expansion is restricted to the bone marrow compartment. However, once eosinophils "escape" the developmental regulation by PIRs and enter the blood, PIR-B is capable of suppressing eosinophil migration in response to eotaxins (15). This notion is reinforced by this study's microarray data demonstrating a tissue-specific suppressive function for PIR-B (in terms of IL-13–regulated

Table I. Genes of interest that were upregulated in eosinophils in the esophagus compared with the bone marrow of *CC10-Il13*^{Tg}/*Pirb*$^{+/+}$ mice

	Gene Symbol	Fold Change (Esophagus/Bone Marrow)
Surface molecules	*Ccrl2*	29.3
	Gp49a	16.1
	Il1r2	6.97
	Cd300ld	6.36
	Ccr1	3.38
	Cd300lf	3.22
	Cd300lb	2.96
	Lilrb3	2.90
	Lilra6	2.79
	Csf2rb2	2.78
Cell adhesion and migration molecules	*Itga2*	3.07
	Itga4	2.75
	Cd44	2.61
Enzymes	*Ptgs2*	74.8
	Ear11	50.7
	Adam8	6.42
	Mmp25	2.54
Secreted factors	*Il1a*	34.9
	Il1b	21.0
	Cxcl2	20.8
	Tnfaip3	15.6
	Ccl3	11.8
	Ccl2	5.76
	Retnlg	5.43
	Il4	5.40
	Retnla	3.87
	Postn	3.60
	Csf1	2.59
	Ccl4	2.08
Intracellular signal molecules	*Nfkbiz*	7.63
	Nfkbia	3.47
	Nfkbie	2.44
	Mapkapk2	2.30
	Junb	2.30
	Cebpb	2.27
	Mapk6	2.24
	Mapk1ip1	2.06
MicroRNA	*Mir1931*	16.8
	Mir146b	3.64
	Mir21	2.75
Cell cycle molecules	*G0s2*	7.09
	Ccng2	4.75
	S100a4	3.72
	Gadd45a	3.50
	S100a10	2.61
Survival molecule	*Bcl2l11*	6.59
	Fas	5.83

gene expression) in the esophagus but not the bone marrow. In addition, IL-13 induces eosinophilic inflammation via the generation of a strong chemotactic gradient for eosinophil recruitment independently of increasing the level of IL-5. We demonstrated recently that PIR-B is a negative regulator of eosinophil chemotaxis in response to eotaxins (15). Consistently, *CC10-Il13*^{Tg}/*Pirb*$^{-/-}$ mice express comparable levels of eotaxins to those found in *CC10-Il13*^{Tg}/*Pirb*$^{+/+}$ mice. Yet, they still display markedly increased infiltration of eosinophils in the lungs and esophagus. Collectively, this suggests that *Pirb*$^{-/-}$ eosinophils hypermigrate in response to eotaxins, as we showed previously (15).

Global microarray analyses revealed that IL-13–elicited esophageal eosinophils express multiple genes that are associated with fibrosis and tissue remodeling (e.g., *Adam8*, *Ear11*, *Arg2*, *Mmp25*, *Ecm1*, *Retnla*, *Postn*, *Il1a*, *Il1b*, and *Hif1a*). Although these data are limited by the fact that we could not compare the genetic signature of IL-13–induced esophageal eosinophils with naive esophageal eosinophils, it is important to note that the inflammatory conditions that promoted tissue eosinophilia were associated with increased IL-13 (3, 4, 19) and that the normal esophagus is devoid of eosinophils. Thus, our results may reflect the genetic signature of eosinophils under disease conditions.

One of the notable findings of our study was that *CC10-Il13*^{Tg}/*Pirb*$^{-/-}$ mice display markedly increased tissue remodeling. This finding is of specific interest because structural cells, such as epithelial cells, fibroblasts, and endothelial cells, do not express PIR-B. Thus, the increased tissue remodeling in *CC10-Il13*^{Tg}/*Pirb*$^{-/-}$ mice may be due to the lack of PIR-B's negative regulation of IL-13–mediated responses in a PIR-B^{+} cell type. Our findings suggest that PIR-B is a key negative regulator of eosinophil effector functions and may offer an explanation for the lack of eosinophil-dependent pathology in IL-13–transgenic mice (4). In fact, our finding suggests that expression of PIR-B in eosinophils may be sufficient to dampen their pathological activities in the esophagus. Indeed, the expression of PIR-B in the esophagus was predominantly associated with its expression in eosinophils, and *CC10-Il13*^{Tg}/*Pirb*$^{-/-}$ mice display increased eosinophilic infiltration to the esophagus, which was associated with increased tissue remodeling. In support of this notion, eosinophils express various profibrogenic mediators, including MMPs, TIMPs, VEGF, TGF-β, FGF, and CCL18. Furthermore, clinical and experimental studies using eosinophil-deficient or hypereosinophilic mice tightly link eosinophils with tissue remodeling in numerous diseases, including asthma and EoE. Thus, loss of PIR-B's negative regulation in eosinophils may result in increased tissue remodeling. Indeed, using ERK phosphorylation as a surrogate marker for eosinophil activation, we clearly show that PIR-B negatively regulates ERK phosphorylation in response to the IL-13–induced esophageal microenvironment. Furthermore, microarray analyses on primary *Pirb*$^{-/-}$ esophageal eosinophils demonstrated a distinct genetic signature that was associated with a hyperactivated eosinophil phenotype. For example, genes of TGF-β signaling molecules that promote epithelial growth, fibrosis, and tissue remodeling (i.e., *Bmpr2*, *Bmp2*, *Tgfbi*, and *Smad3*), as well as various factors that promote epithelial to mesenchymal transition (a recent pathway identified in EoE) and fibrosis (i.e., *Notch1*, *Notch2*, *Mmp9*, *Adam19*, and *Areg*), had increased expression in *Pirb*$^{-/-}$ cells (2, 20–22). Integration of the ERK phosphorylation data and genetic signature analysis suggests that increased pathology in *CC10-Il13*^{Tg}/*Pirb*$^{-/-}$ mice is not merely due to increased eosinophil numbers in the tissue; it is also attributed to the fact that these eosinophils are hyperactivated.

Collectively, we demonstrate an inhibitory role for PIR-B in the regulation of esophageal eosinophil recruitment and activation, as well as the consequent esophageal pathology, in response to IL-13 induction. Given the involvement of IL-13 in EoE and additional

Table II. Genes of interest that were upregulated in eosinophils of the esophagus compared with the bone marrow of *CC10-Il13*^{Tg}/*Pirb*$^{+/+}$ and *CC10-Il13*^{Tg}/*Pirb*$^{-/-}$ mice

Gene Symbol	*Pirb*$^{+/+}$	*Pirb*$^{-/-}$	Fold Change (*Pirb*$^{-/-}$/*Pirb*$^{+/+}$)
Adamdec1	3.15	16.0	5.08
Btg2	5.44	22.0	4.03
Cxcl3	8.84	30.9	3.49
Retnla	3.87	13.3	3.43
Irg1	13.2	41.9	3.17
Csf1	2.59	7.53	2.91
Pla2g7	4.20	9.90	2.36
Ccr1	3.38	7.92	2.34
Lilra6	2.79	6.46	2.31

Table III. Genes of interest that were upregulated in eosinophils of the esophagus compared with the bone marrow in *CC10Il13*^{Tg}*/Pirb*$^{-/-}$mice but not in *CC10Il13*^{Tg}*/Pirb*$^{+/+}$mice

	Gene Symbol	Fold Change (Esophagus/Bone Marrow)
Surface molecules	*Il5ra*	5.73
	Il12rb2	4.24
	Notch2	3.69
	Notch1	2.58
	Bmpr2	2.52
	Ifnar1	2.28
	Cd300a	2.61
Cell adhesion and migration molecules	*Itgax*	6.04
	Itgb3	4.67
	Itgal	3.75
	Vasp	3.21
	Ezr	2.84
	Acta1	2.75
	Cd24a	2.07
Enzymes	*Capn2*	5.66
	Mmp9	3.49
	Adam19	2.73
Secreted factors	*Il6*	18.9
	Tnf	5.72
	Cxcl10	4.43
	Tgfbi	4.42
	Ccl8	3.84
	Areg	2.18
Intracellular signaling molecules	*Jun*	3.72
	Stat6	3.44
	Nfkb2	2.90
	Tnik	2.71
	Rela	2.69
	Fosl1	2.35
	Jak2	2.25
	Nfkbib	2.24
	Irak2	2.03
MicroRNA	*Mir1957*	9.22
	Mir142	8.29
Cell cycle molecules	*Gadd45b*	5.63
	S100a6	2.09
Survival molecule	*Bcl10*	2.20

allergic diseases, the identification of an IL-13–dampening loop that is dependent upon PIR-B may have implications for human disease, because PIR-B human orthologs are readily expressed by eosinophils (23). These data provide new understanding of the signaling mechanisms that restrict eosinophil functions in EoE and may provide new therapeutic targets for combating it.

Acknowledgments

We thank H. Kubagawa (University of Alabama, Tuscaloosa, AL) for providing *Pirb*$^{-/-}$ mice, Dr. Jamie Lee (Mayo Clinic, Scottsdale, AZ) for the anti-MBP reagent, and Shawna Hottinger for editorial assistance.

Disclosures

M.E.R. is a consultant for Immune Pharmaceuticals, Receptos, NKT Therapeutics, Genetech/Roche, and Novartis. He has equity interest in Immune Pharmaceuticals, Celsus Therapeutics, Receptos, and NKT Therapeutics, as well as royalty rights to reslizumab being developed by Teva Pharmaceuticals. A.M. is a consultant for Compugen and Augmanity Nano Ltd. The other authors have no financial conflicts of interest.

References

1. Rothenberg, M. E. 2009. Biology and treatment of eosinophilic esophagitis. *Gastroenterology* 137: 1238–1249.
2. Aceves, S. S., R. O. Newbury, R. Dohil, J. F. Bastian, and D. H. Broide. 2007. Esophageal remodeling in pediatric eosinophilic esophagitis. *J. Allergy Clin. Immunol.* 119: 206–212.
3. Blanchard, C., M. K. Mingler, M. Vicario, J. P. Abonia, Y. Y. Wu, T. X. Lu, M. H. Collins, P. E. Putnam, S. I. Wells, and M. E. Rothenberg. 2007. IL-13 involvement in eosinophilic esophagitis: transcriptome analysis and reversibility with glucocorticoids. *J. Allergy Clin. Immunol.* 120: 1292–1300.
4. Zuo, L., P. C. Fulkerson, F. D. Finkelman, M. Mingler, C. A. Fischetti C. Blanchard, and M. E. Rothenberg. 2010. IL-13 induces esophageal remodeling and gene expression by an eosinophil-independent, IL-13R alpha 2-inhibited pathway. *J. Immunol.* 185: 660–669.
5. Fulkerson, P. C., C. A. Fischetti, L. M. Hassman, N. M. Nikolaidis, and M. E. Rothenberg. 2006. Persistent effects induced by IL-13 in the lung. *Am. J. Respir. Cell Mol. Biol.* 35: 337–346.
6. Rothenberg, M. E., T. Wen, A. Greenberg, O. Alpan, B. Enav, I. Hirano, K. Nadeau, S. Kaiser, T. Peters, A. Perez, et al. 2015. Intravenous anti-IL-13 mAb QAX576 for the treatment of eosinophilic esophagitis. *J. Allergy Clin. Immunol.* 135: 500–507.
7. Munitz, A. 2010. Inhibitory receptors on myeloid cells: new targets for therapy? *Pharmacol. Ther.* 125: 128–137.
8. Kubagawa, H., C. C. Chen, L. H. Ho, T. S. Shimada, L. Gartland, C. Mashburn, T. Uehara, J. V. Ravetch, and M. D. Cooper. 1999. Biochemical nature and cellular distribution of the paired immunoglobulin-like receptors, PIR-A and PIR-B. *J. Exp. Med.* 189: 309–318.
9. Kubagawa, H., P. D. Burrows, and M. D. Cooper. 1997. A novel pair of immunoglobulin-like receptors expressed by B cells and myeloid cells. *Proc. Natl. Acad. Sci. USA* 94: 5261–5266.
10. Ujike, A., K. Takeda, A. Nakamura, S. Ebihara, K. Akiyama, and T. Takai. 2002. Impaired dendritic cell maturation and increased T(H)2 responses in PIR-B($^{-/-}$) mice. *Nat. Immunol.* 3: 542–548.
11. Wheadon, H., N. R. Paling, and M. J. Welham. 2002. Molecular interactions of SHP1 and SHP2 in IL-3-signalling. *Cell. Signal.* 14: 219–229.
12. Mitsuhashi, Y., A. Nakamura, S. Endo, K. Takeda, T. Yabe-Wada, T. Nukiwa, and T. Takai. 2012. Regulation of plasmacytoid dendritic cell responses by PIR-B. *Blood* 120: 3256–3259.
13. Ben Baruch-Morgenstern, N., D. Shik, I. Moshkovits, M. Itan, D. Karo-Atar, C. Bouffi, P. C. Fulkerson, D. Rashkovan, S. Jung, M. E. Rothenberg, and A. Munitz. 2014. Paired immunoglobulin-like receptor A is an intrinsic, self-limiting suppressor of IL-5-induced eosinophil development. *Nat. Immunol.* 15: 36–44.
14. Ma, G., P. Y. Pan, S. Eisenstein, C. M. Divino, C. A. Lowell, T. Takai, and S. H. Chen. 2011. Paired immunoglobin-like receptor-B regulates the suppressive function and fate of myeloid-derived suppressor cells. *Immunity* 34: 385–395.
15. Munitz, A., M. L. McBride, J. S. Bernstein, and M. E. Rothenberg. 2008. A dual activation and inhibition role for the paired immunoglobulin-like receptor B in eosinophils. *Blood* 111: 5694–5703.
16. Karo-Atar, D., I. Moshkovits, O. Eickelberg, M. Königshoff, and A. Munitz. 2013. Paired immunoglobulin-like receptor-B inhibits pulmonary fibrosis by suppressing profibrogenic properties of alveolar macrophages. *Am. J. Respir. Cell Mol. Biol.* 48: 456–464.
17. Chu, V. T., A. Fröhlich, G. Steinhauser, T. Scheel, T. Roch, S. Fillatreau, J. J. Lee, M. Löhning, and C. Berek. 2011. Eosinophils are required for the maintenance of plasma cells in the bone marrow. *Nat. Immunol.* 12: 151–159.
18. Zimmermann, N., M. L. McBride, Y. Yamada, S. A. Hudson, C. Jones, K. D. Cromie, P. R. Crocker, M. E. Rothenberg, and B. S. Bochner. 2008. Siglec-F antibody administration to mice selectively reduces blood and tissue eosinophils. *Allergy* 63: 1156–1163.
19. Rothenberg, M. E. 2004. Eosinophilic gastrointestinal disorders (EGID). *J. Allergy Clin. Immunol.* 113: 11–28, quiz 29.
20. Shao, J., and H. Sheng. 2010. Amphiregulin promotes intestinal epithelial regeneration: roles of intestinal subepithelial myofibroblasts. *Endocrinology* 151: 3728–3737.
21. Leask, A., and D. J. Abraham. 2004. TGF-beta signaling and the fibrotic response. *FASEB J.* 18: 816–827.
22. Cheng, E., R. F. Souza, and S. J. Spechler. 2012. Tissue remodeling in eosinophilic esophagitis. *Am. J. Physiol. Gastrointest. Liver Physiol.* 303: G1175–G1187.
23. Tedla, N., C. Bandeira-Melo, P. Tassinari, D. E. Sloane, M. Samplaski, D. Cosman, L. Borges, P. F. Weller, and J. P. Arm. 2003. Activation of human eosinophils through leukocyte immunoglobulin-like receptor 7. *Proc. Natl. Acad. Sci. USA* 100: 1174–1179.